Surface Science 678 (2018) 169–176

Contents lists available at ScienceDirect

Surface Science

journal homepage: www.elsevier.com/locate/susc

Effect of adsorbates on single-molecule junction conductance

H. Okuyama*[,a], H. So[a], S. Hatta[a], T. Frederiksen[b,c], T. Aruga[a]

[a] Department of Chemistry, Graduate School of Science, Kyoto University, Kyoto 606-8502, Japan
[b] Donostia International Physics Center (DIPC), 20018 San Sebastián, Spain
[c] IKERBASQUE, Basque Foundation for Science, 48013 Bilbao, Spain

ARTICLE INFO

Keywords:
Scanning tunneling microscope
Single-molecule junction
Cu surface
Molecular conductance

ABSTRACT

Electronic conduction through molecular junctions depends critically on the electronic state at the anchor site, suggesting that local reactions on the electrodes may play an important role in determining the transport properties. However, single-molecule junctions have never been studied with the chemical states of the electrodes controlled down to the atomic scale. Here, we study the effect of surface adsorbates on the molecular junction conductance by using a scanning tunneling microscope (STM) combined with density functional theory (DFT) and nonequilibrium Green's function (NEGF) calculations. By vertical control of a STM tip over a phenoxy (PhO) molecule on Cu(110), we can lift and release the molecule against the tip, and thus reproducibly control a molecular junction. Using this model system, we investigate how the conductance changes as the molecule is brought to the vicinity of oxygen atoms or a hydroxyl group chemisorbed on the surface. This proximity effect of surface adsorbates on the molecular conductance is simulated by DFT-NEGF calculations.

1. Introduction

Scanning tunneling microscopes (STM) have been used not only to image individual molecules on the surface, but also to manipulate them for studying single-molecule dynamics and chemistry [1,2]. A Xe atom on Ni(110) was transferred from the surface to the STM tip and vice versa, realizing the smallest switch consisting of a single atom [3]. A carbon monoxide (CO) molecule was also successfully transferred between the STM tip and metal surfaces [4], which was used to prepare a "molecular tip" for high-resolution surface imaging [5,6]. Such control of single atoms or molecules with the tip is called vertical manipulation. More recently, vertical manipulation was employed to make a molecular bridge in the STM gap: one end of a molecule is lifted up to the STM tip while the other end is bonded to the surface, giving rise to a single-molecule junction between two electrodes (tip and surface). This control enabled precise studies of single-molecule junctions such as the role of contact spacing and molecular tilt angle [7], conductance as a function of molecular length [8], tuning of Kondo resonances [9], and electroluminescence [10]. Apart from these applications, the STM tip was also used to manipulate individual molecules along the surface. The precise control of the interaction between tip and adsorbate enables one to move atoms [11–13] or molecules [14–16] to the desired position on the surface without rupturing the atom (molecule)-surface bond. This is called lateral manipulation. The tip-molecule interaction is significant when they are brought in close vicinity. By controlling the distance between the tip and molecule, the molecule is pulled or pushed by the tip as it is moved along the surface, depending on the nature of the interaction (attractive or repulsive).

In our previous works using vertical manipulation [17,18] we presented reversible control of single-molecule junctions by attaching the STM tip to a phenoxy (C_6H_5O, PhO) molecule bonded to the Cu(110) surface. PhO is adsorbed on Cu(110) in a nearly flat configuration [19] and is reversibly lifted (released) to (from) the STM tip while it is anchored to the surface via a chemical bond to the oxygen atom. Using this reversible junction control, we revealed the influence of the anchor and side groups [17] on the single-molecule junction conductance. Furthermore, by using lateral manipulation of the molecule, the effect of molecule-molecule interaction on the conductance was studied, where the reduction of the conductance by as large as ~ 50% was observed for a molecule confined in an island [18]. These results suggests that the environment is an essential factor for determining the transport properties of single-molecule junctions. Here, we study the impact of surface adsorbates, i.e., how nearby oxygen atoms or a hydroxyl group on the surface influence the conductance of the junction. By precisely controlling the distance between a PhO molecule and the adsorbates on the surface, we reveal that the conductance can be reduced by up to ~ 30% depending on the distance. This result explicitly shows that electron transport through molecular junctions is sensitive to the atomic-scale oxidation of the electrode.

* Corresponding author.
E-mail address: hokuyama@kuchem.kyoto-u.ac.jp (H. Okuyama).

https://doi.org/10.1016/j.susc.2018.04.024
Received 30 January 2018; Received in revised form 25 April 2018; Accepted 30 April 2018
Available online 16 May 2018
0039-6028/

2. Methods

The experiments were performed in an ultra-high vacuum chamber equipped with STM operating at 4.5 K. The Cu(110) surface was cleaned by repeated cycles of argon ion sputtering and annealing. The surface was first exposed to phenol vapor at 300 K, giving rise to partial dehydrogenation to PhO species on the surface [19]. The surface was then exposed to molecular oxygen at 78 K. An oxygen molecule was dissociated to produce two atomic species at the hollow sites on the surface, which were imaged as two neighboring depressions by STM [20]. To be specific, oxygen atoms were produced most frequently along the $[1\bar{1}0]$ direction at an interval of $2a_0$, where a_0 represents the atomic distance of the Cu(110). This trend was similar between the adsorption at 4 K [20] and that at 78 K in the present work. We studied the interaction of PhO with oxygen atoms in this configuration. The hydroxyl groups were introduced on the surface by exposing the surface to water vapor and dissociating the water molecules by voltage pulses under STM tip [21]. The STM images were obtained at sample bias $V = 50$ mV and tunnel current $I = 1$ nA. The sample bias was maintained at $V = 50$ mV during the vertical and lateral manipulations. Electrochemically etched tungsten tips were used as an STM probe. The tips were repeatedly and gently touched to the Cu surface to coat them with copper, to prepare Cu-terminated tips for reliable switching of the junction [18].

The bonding structure of PhO was determined by density functional theory (DFT) calculations (Figs. 1b and 2b) using Siesta [22] and the vdw-DF2 van der Waals functional [23–25]. The unit cell consists of a 5×6 Cu(110) surface slab with 13 atomic layers (lattice constant $a = 3.64$ Å). A 300 Ry energy cutoff was used for the real-space integrations together with a $2 \times 2 \times 1$ k-mesh for the Brillouin zone sampling. We used a long-ranged double-ζ plus polarization (DZP) basis set for the C, H, O, S and Cu surface layer and tip atoms and a short-ranged single-ζ plus polarization (SZP) basis set for the bulk Cu atoms. The molecule, the two topmost surface layers, and the four Cu apex atoms were relaxed until residual forces were smaller than 0.02 eV/Å. The structure of the junction with O and OH species in the vicinity was also calculated, showing the similar configuration of the molecular junction as that without them. Electron transmission was computed with the nonequilibrium Green's function (NEGF) method as implemented in the DFT-NEGF code TranSiesta [26,27] using a 21×21 k-mesh. We note that this computational approach differs slightly from that employed in our previous works [17,18], most notably that the geometry is determined with Siesta in a larger simulation cell and that electron transport is evaluated here with the vdW-DF2 functional [23–25]. Quantitatively the transmission near the Fermi level is unchanged, but a downshift of the LUMO state of about 0.5 eV is observed. Our previous result[17] for PhO in the smaller 4×5 unit cell and identical tip position is included in gray in Fig. 6e for direct comparison.

3. Results and discussion

Fig. 1a shows the experimental STM image of a PhO molecule on Cu (110). The image consists of a protrusion and a smaller depression. The adsorbed state of PhO on Cu(110) was previously studied by electron energy loss spectroscopy [19]. The spectra exhibited the intense peaks due to C–H wagging mode of the phenyl ring, suggesting that the ring was lying flat on the surface. As shown in Fig. 1b, the relaxed structure from DFT shows that the PhO species is bonded to the short-bridge site via oxygen atom and aligned along the [001] direction with the phenyl ring tilted by 22° from the surface plane. The protrusion and depression in the STM image of Fig. 1a can be associated with the density of states at the phenyl ring and oxygen atom of PhO, respectively.

As described previously the PhO molecule can be lifted up to the STM tip by vertical manipulation [17,18] with the following procedure: First, the tip was positioned precisely over the protrusion of the STM image [Fig. 1(a)] by using tracking routine at $V = 50$ mV and $I = 1$ nA. After the feedback was turned off, the tip was laterally displaced toward the depression by 1–3 Å. This is the initial position and the height was defined as $\Delta z = 0$. Then, the tip was approached toward the molecule (increase of Δz) and the tunnel current was recorded during the approach and subsequent retract ($I - \Delta z$ curve). In the meantime, the bias voltage was maintained at $V = 50$ mV. Typical results are shown in Fig. 2a: During the approach (black curves), the current jumps at around $\Delta z = 2$ Å, where the molecule is lifted and contacted with the tip via phenyl ring while it is anchored to the surface via oxygen atom thus forming a molecular junction. The dependence on the lateral displacement was mentioned in our previous report [18], and the larger displacement caused longer hysteresis in the switching curve. The data in Fig. 2 was obtained with lateral displacement of 2 Å. The structure of the lifted configuration is shown in Fig. 2b (on-state), as calculated by the DFT calculations [17,18]. Subsequently, during the retraction of the tip (red curves), the phenyl ring is released to the surface at around $\Delta z = 1$ Å, and the initial state in Fig. 1 (off-state) is recovered in the end. In this way, a molecular junction is controlled reversibly by bi-directional motion of a phenyl ring between the surface and the tip. It is noted that the tip apex as well as the molecule is not perturbed before and after the junction formation, as ensured from the STM images

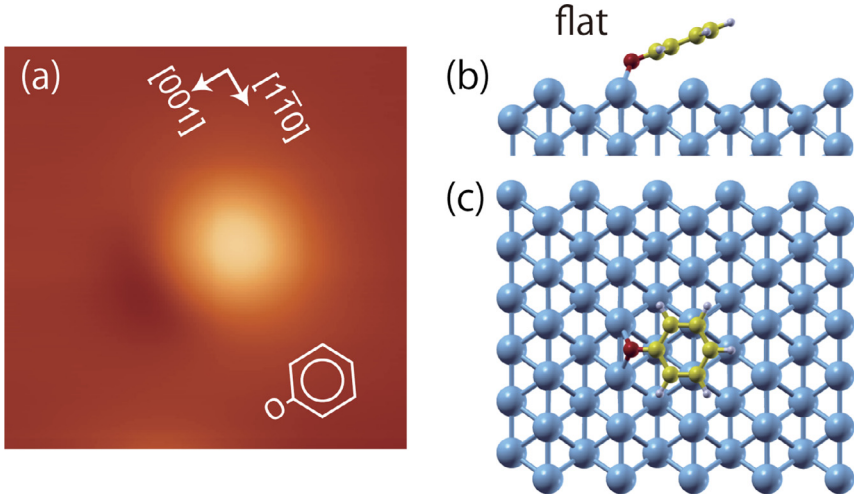

Fig. 1. (a) STM image of a PhO molecule on Cu(110) (23 Å × 23 Å, $V = 50$ mV and $I = 1$ nA). The image consists of a protrusion and depression which are associated with the density of states of phenyl ring and oxygen atom, respectively. (b) The bonding structure of a PhO molecule to Cu(110) obtained by DFT.

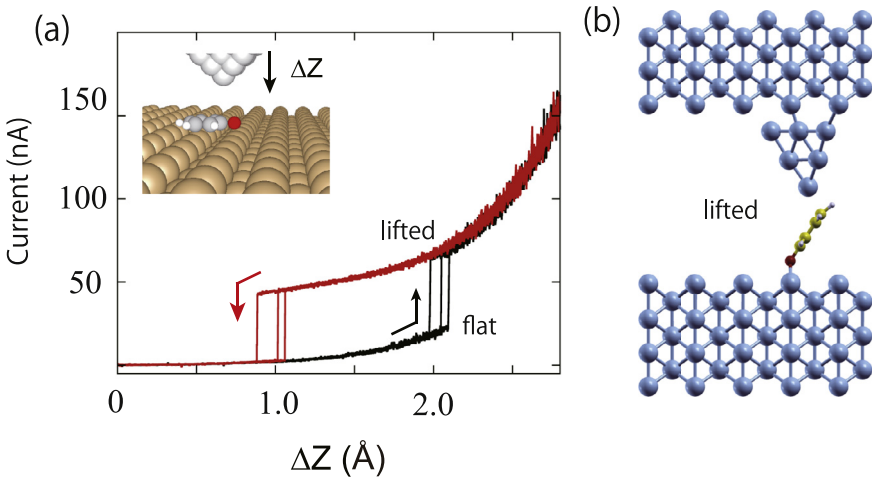

Fig. 2. (a) Typical tunnel current recorded during repeated approach (black) and retraction (red) of the tip along the surface normal above a PhO molecule on Cu (110). Before approach, the lateral tip position was adjusted over the protrusion in Fig. 1(a) by iterative tracking routine at $V = 50$ mV and $I = 1$ nA. Then the feedback was turned off and the tip was offset by 2 Å in the [001] direction (toward oxygen side), where the tip position was defined as $\Delta z = 0$. Subsequently, the tip was approached with $V = 50$ mV and the current was recorded. The increase of Δz corresponds to the approach toward the molecule. The two-state switching of the current was observed due to the bidirectional motion of a phenyl ring between the surface and the tip. (b) The calculated structure of a PhO molecule on Cu(110) lifted to the STM tip. (For interpretation of the references to color in this figure legend, the reader is referred to the web version of this article.)

obtained before and after the manipulation (see Supplementary Information, Fig. S1). This reversibility enables us to reproduce identical molecular junctions at the atomistic level and to repeat the switching with the conductance kept constant, as shown in Fig. 2a where the switching was repeated three times.

The precise control of a single-molecular junction down to atomic scale is indispensable for reliable evaluation of the junction conductance [28–30]. In previous works, the conductance through single-molecule junctions was thoroughly investigated by break-junction experiments as a function of the molecular structure [31–33] and anchoring groups [34–36]. Another important variable affecting electron transport is the environment of the molecule, although this has received less attention [37,38]. The use of STM for single-molecule junction formation is more reliable in that the at least one electrode (flat surface) is well-defined at atomistic level and also that the junction can be formed in a non-destructive way [39–46]. In our setup, the Cu surface is well-defined, making it feasible to study the junction with its environment on that electrode controlled at atomistic level [18]. The molecular conductance of the junction can be derived from the abrupt decrease (height of the staircase) in the tunnel current when the junction is released (Fig. 2a). We note that the conductance value depends on the tip apex and thus varies from tip to tip [17]. Nevertheless, the conductance is constant during the repeated junction formation/release as far as tip apex is maintained intact, as described above. Therefore it is possible to compare the conductance of the same PhO molecule positioned in different environmental conditions on the surface.

We utilized lateral manipulation of a PhO molecule to move it to the desired position on the surface (Fig. S1). The PhO molecule can be displaced along the $[1\bar{1}0]$ direction of the surface in the lift-and-drag manner [18]. First, one of the PhO molecules was lifted to the tip to form a molecular junction, as described above. Subsequently the tip was translated in the $[1\bar{1}0]$ direction at constant height while the junction was maintained. After the translation, the tip was retracted and the molecule was released to the surface. This manipulation procedure resulted in the stepwise displacement of the molecule along the $[1\bar{1}0]$ direction. Note that the orientation of the molecule was not changed between the manipulations as long as the tip was displaced along the $[1\bar{1}0]$ direction. The tunnel current during the translation of the tip shows characteristic saw-tooth shape (Fig. S1), where individual jumps are associated with the hopping of the molecule from site to site. This is different from previous, related manipulations [11–16] in that the tip is in contact with the molecule during the lateral manipulation and thus the molecule is dragged while it is *on* the tip.

The electron transport through a molecular junction depends critically on the local density of states at the molecule/electrode binding site, and thus, it is essential to control the structure and electronic states of the electrode in atomic-scale precision for microscopic understanding of the conductance through the junction. In particular, electrodes are readily oxidized by the reaction with molecular oxygen or water vapor when it works under ambient conditions, which would significantly affect the density of states and thus the conducting property of the molecular junctions. Here, we investigate the effect of oxygen atoms adsorbed on the surface on the conductance of a PhO molecule.

Fig. 3a shows the STM image of two oxygen atoms coadsorbed near the PhO molecule on Cu(110). The lattice of Cu(110) (white lines) was depicted according to the positions of the PhO [19]. There existed some PhO molecules outside the cut images of Fig. 3a–d, which allowed us to depict the lattice in a reliable way. Accordingly, two oxygen atoms were located at the hollow sites (white dots), in line with the previous result [20]. Note that the oxygen atoms are imaged as one elongated depression; they are not resolved in the height profile because of the short O–O distance ($2a_0$).

By the lateral manipulation, we varied the position of the PhO molecule with respect to the oxygen atoms on the surface (Fig. 3a–e). The $I - \Delta z$ curves were recorded for each configuration (Fig. S2), from which the conductance was obtained (Fig. 3f). The conductance is presented by the ratio to that for an isolated PhO. Typical traces for the configurations in Fig. 3a and d are shown in Fig. 3g, where the measurements were repeated five times for each. Obviously, a conductance reduction by 10% is discernible when the molecule is brought to the vicinity of the oxygen pair (Fig. 3d). Note that the oxygen adatom on the surface is not involved in the contact but placed nearby the junction just perturbing the conductance. We also note that the baseline in

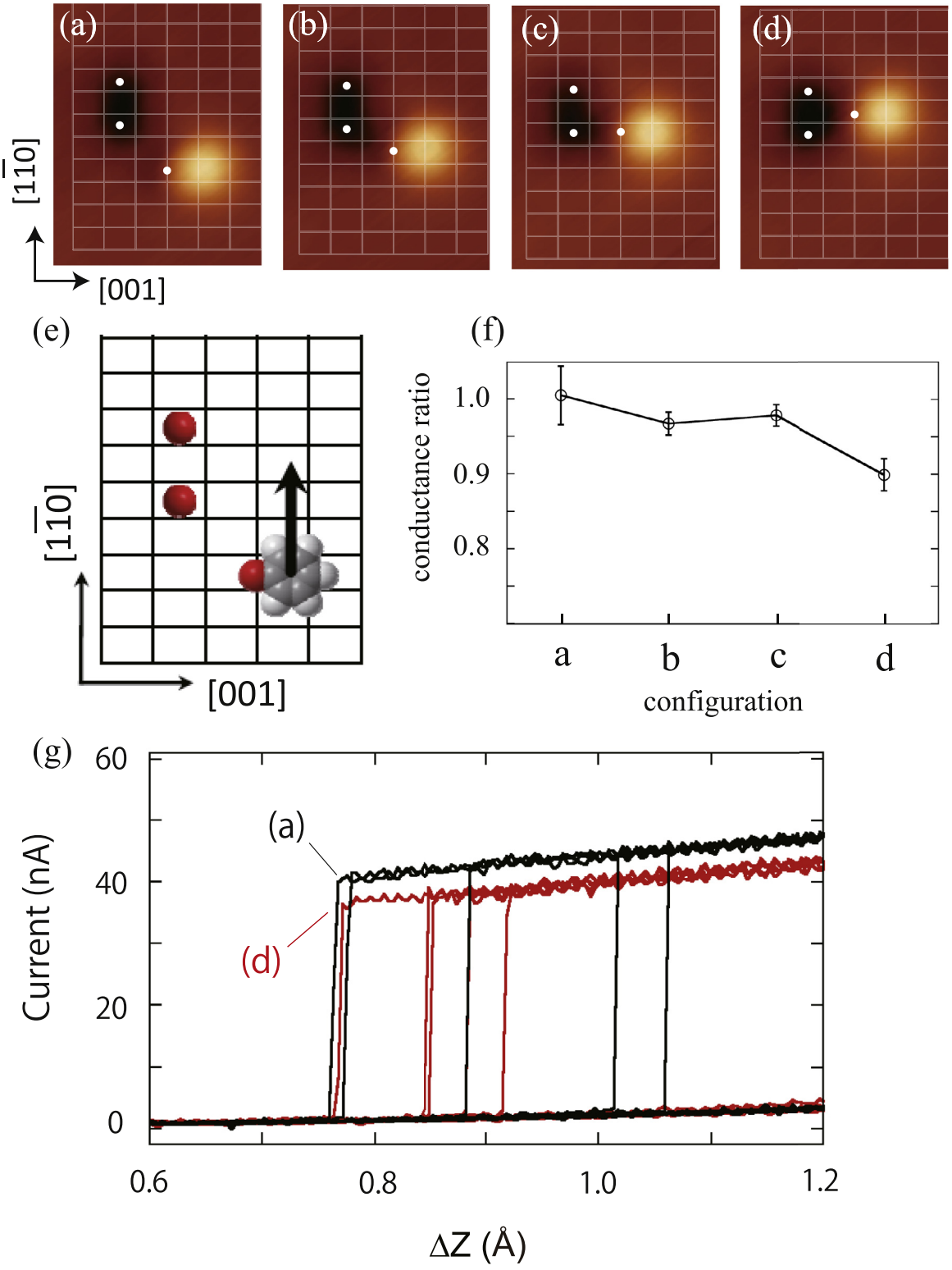

Fig. 3. (a)–(d) The STM images of a PhO molecule and oxygen pair (elongated depression) on Cu(110) in various configurations. The white lines and dots represent the lattice of Cu(110) and the position of oxygen atoms, respectively. (e) The illustration for the configuration (a) and the way the molecule was brought to the positions corresponding to (b)–(d). (f) The corresponding conductance values obtained at $V = 50$ mV, indicating that the conductance depends on the distance from the oxygen pair. The measurements were repeated by five cycles for each. (g) The black and red represent typical $I - \Delta z$ curves obtained for the configurations (a) and (d), respectively (recorded five times for each, $V = 50$ mV). (For interpretation of the references to color in this figure legend, the reader is referred to the web version of this article.)

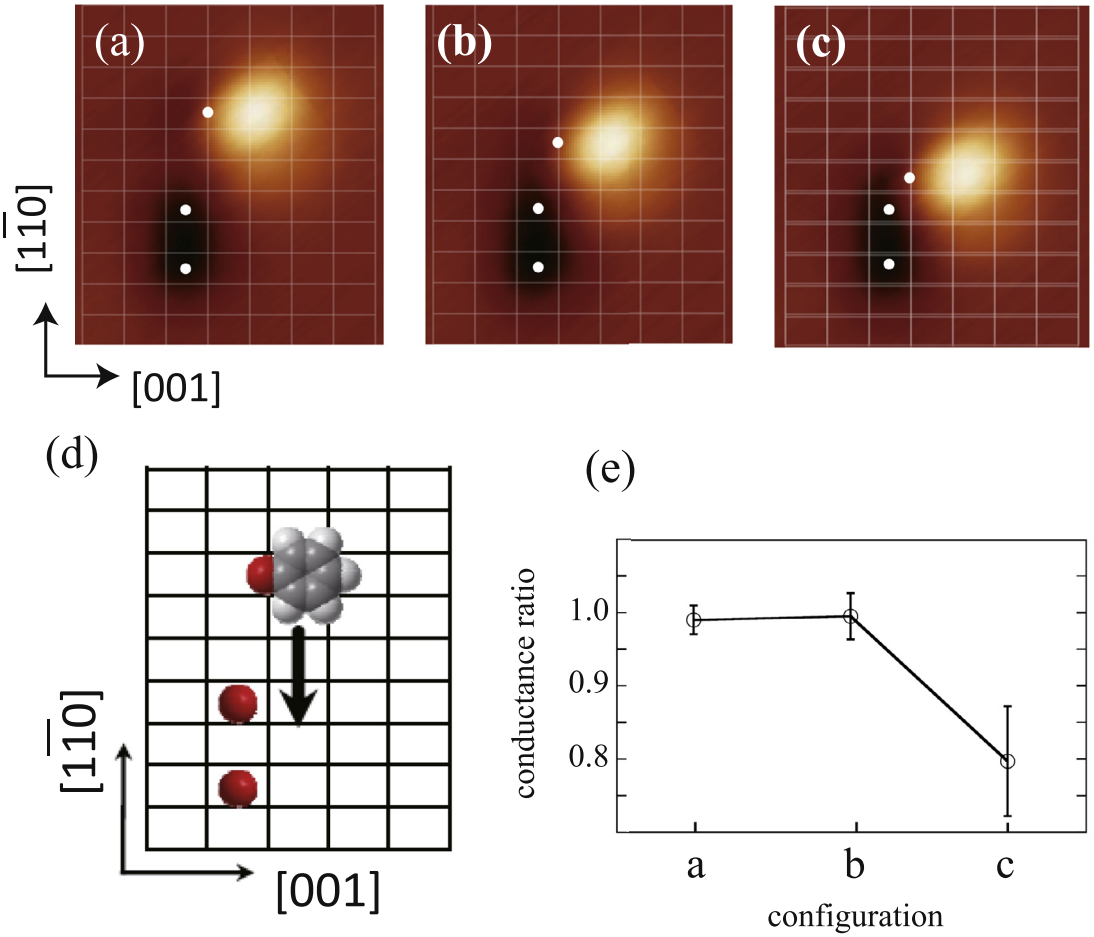

Fig. 4. (a)–(c) The STM images of a PhO molecule and oxygen pair on Cu(110) at various distances. The white dots indicate the position of oxygen atoms. (d) The illustration for the configuration (a) and the way the molecule was brought to the positions corresponding to (b) and (c). (e) The corresponding conductance values ($V = 50$ mV).

Fig. 3g represents the current as the tip approaches the PhO while it is on the surface (before lift). The same baseline indicates that the conductance through the molecule without lift is almost equal for (a) and (d). Thus, it is the conductance through the lifted molecule (junction) that is influenced by the presence of oxygen atoms.

Similarly, Fig. 4a–c show the STM images of PhO on the atomic row and oxygen pair now in the *adjacent* trough, as depicted in Fig. 4d. In this configuration, the conductance for PhO positioned at various distances from the oxygen pair (Fig. 4e) shows a reduction by up to 20% when the molecule is brought to the nearest neighbor site (Fig. 4c). The corresponding $I - \Delta z$ curves are shown in Fig. S3. The adsorption of electronegative oxygen atoms may reduce the local density of states at the Fermi level of metal surfaces [47], which would be expected to affect the density of states at the anchoring site and decrease the conductance of a molecule placed in the vicinity, as discussed below in details. It is noted that further approach of the PhO molecule from Fig. 4c induced the oxygen atom to be displaced to the next hollow site along the trough, suggesting repulsive interaction between them at this distance.

A OH species is a fundamental oxidation product under wet condition, and thus may influence the transport property of molecular junctions fabricated in electrolyte solution. Fig. 5 shows the STM images of PhO before and after it was translated to the vicinity of an OH group. The OH group is bonded to the short-bridge site on the atomic row and appears as “ring” depressions (Fig. 5a) [21]. When the PhO molecule is brought to the vicinity of a OH group (Fig. 5b and d), the conductance is observed to decrease by 30% (Fig. 5c). As in the case of the vicinity effect by oxygen atoms described above, the electronegative OH group on Cu(110) [48] may reduce the local density of states and as a result, decreases the conductance through a molecule placed nearby. In addition, the OH group has a dipole moment which may influence the density of states and thus the conductance of a PhO molecule located nearby [18]. The OH group is adsorbed on Cu(110) with the OH axis tilted and flipped dynamically between two equivalent orientations along [001] [21]. When the oxygen atom of PhO is in the vicinity of OH as shown in Fig. 5d, the flip motion of OH may be quenched with the H atom pointing toward PhO. This is because the oxygen atom of PhO is negatively polarized [18] and the H-bond formation, i.e., O–H...O–Ph, is energetically favorable. Thus, the molecules interact with each other via electrostatic coupling between the polar OH group and the PhO molecule. The electrostatic field induced by the polar OH group causes the orbitals of the conducting PhO molecule to be stabilized, reducing the density of states at the Fermi level [18], and consequently, the conductance decreases.

As the junction conductance is here experimentally evaluated with the environment controlled at an atomic level, it provides an opportunity to test DFT-NEGF methods for the prediction of the environmental effect on the electron transport properties. Our DFT-NEGF

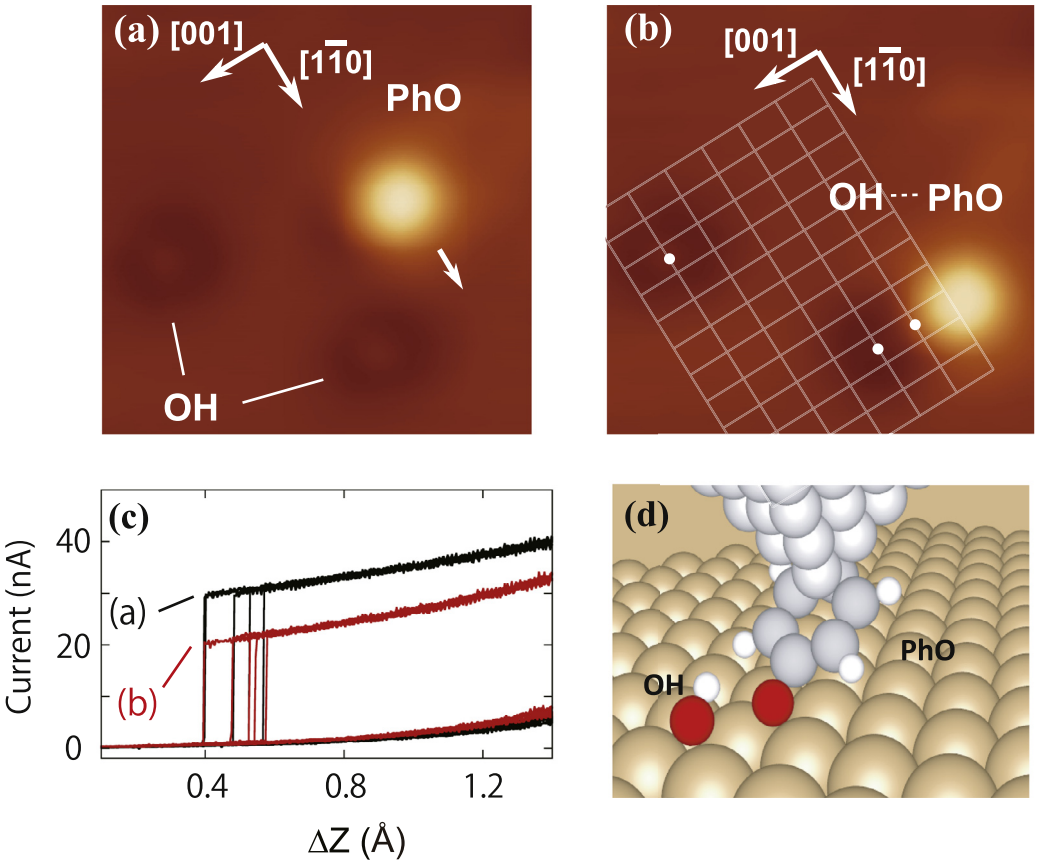

Fig. 5. (a) The STM images of a PhO molecule and OH groups on Cu(110). The latter appears as ring depression. (b) The PhO molecule was translated close to the OH group, and they are located at the next sites along [001]. The white dots indicate the position of oxygen atoms. The image size is 34 Å × 34 Å. (c) Typical $I - \Delta z$ curves at $V = 50$ mV acquired for the configurations (a) and (b), where the conductance is reduced by ~ 30% for the latter (recorded five times for each). (d) The illustration of the lifted PhO for (b), in which the PhO is located at the nearest site to the OH group.

results for the effect of oxygen atoms on the junction conductance are shown in Fig. 6 corresponding to the experimental configurations in Fig. 3. Following our notation in Ref. [17] the tip apex was kept at a fixed location characterized by the height $h = 13.9$ Å and lateral position $x = 1.4$ Å. The characteristic separation between PhO and the individual oxygen atoms in Fig. 6 roughly decreases from panel a to d. The corresponding transport simulations are summarized in Fig. 6e. The low-bias conductance is obtained from the Landauer formula $G = G_0 T(E_F)$, where $G_0 = 2e^2/h$ is the conductance quantum and $T(E) = \mathrm{Tr}[\mathbf{A}_1\boldsymbol{\Gamma}_2]$ is the energy-dependent transmission probability for electrons. Here $\mathbf{A}_1 = \mathbf{G}\boldsymbol{\Gamma}_1\mathbf{G}^\dagger$ is the spectral matrix from electrode 1, $\boldsymbol{\Gamma}_{1(2)}$ the coupling rate to electrode 1 (2), and $\mathbf{G}$ the retarded Green's function for the scattering region. The inset to Fig. 6e shows that the transmission at E_F is reduced by 5% for (d), in qualitative agreement with the experimental result in Fig. 3. However, the overall structure of the transmission curves (e.g., values at $E - E_F = \pm 0.5$ eV) is not systematically varied as the mean distance decreases. This may imply that the environmental effect cannot simply be correlated with the distance due to the anisotropy of the structure and electronic state of the Cu(110) surface. Although the junction becomes rather unstable at high bias voltage beyond $V = \pm 0.2$ V [17], it would be interesting to explore the conductance as a function of V because our simulations indicate a possible dependence of the bias polarity on the conductance in the vicinity of oxygen atoms (i.e., asymmetric ratios in inset to Fig. 6e).

To investigate the origin of the transmission variations with the different oxygen arrangements we show in Fig. 6f the projected density of states (PDOS) from the substrate electrode ($\frac{1}{2\pi}[\mathbf{A}_{\mathrm{sub}}]_{\nu\nu}$ with $\nu \in$ *subset atom*) on the subset of orbitals corresponding to the whole PhO molecule (thick lines) or just the anchoring O-atom (thin lines). The resonances around -1.2 and 2.3 eV in both PDOS and transmission reflect the highest occupied molecular orbital (HOMO) and lowest unoccupied molecular orbital (LUMO), respectively. The PDOS variation between the four different configurations are tiny and better understood by considering the ratios shown in the inset to Fig. 6f. Comparing with Fig. 6e the PDOS ratios correlate well with the transmission ratios. For instance, the PDOS on the anchoring O-atom is slightly reduced going from configuration a to d. This confirms that the DOS at the binding site of the molecule gets slightly reduced by the presence of nearby oxygen atoms, which in turn reduces the conductance. We note that the conductance decrease is not ascribed to geometric effect; the conductance was calculated with the PhO geometry fixed but the other part including two O atoms and the surface relaxed, which reproduced almost the same trend as Fig. 6e and f (Fig. S4).

4. Conclusion

In summary, by vertical control of the STM tip, we lifted and released a PhO molecule on Cu(110) against the tip, thus realizing reversible control of a molecular junction. Using this model system, we address how oxygen atoms or hydroxyl species placed in the vicinity of the junction influence the molecular conductance. Our DFT-NEGF transport calculations reproduced the experimental finding that the conductance is slightly reduced when the molecule is placed near oxygen atoms, related to suppressed density of states at the electrode bonding site. Thus, the atomic-scale control of surface reactions is essential for the understanding of molecular transport properties and provides an opportunity to study the environmental effects of molecular junctions in terms of surface science.

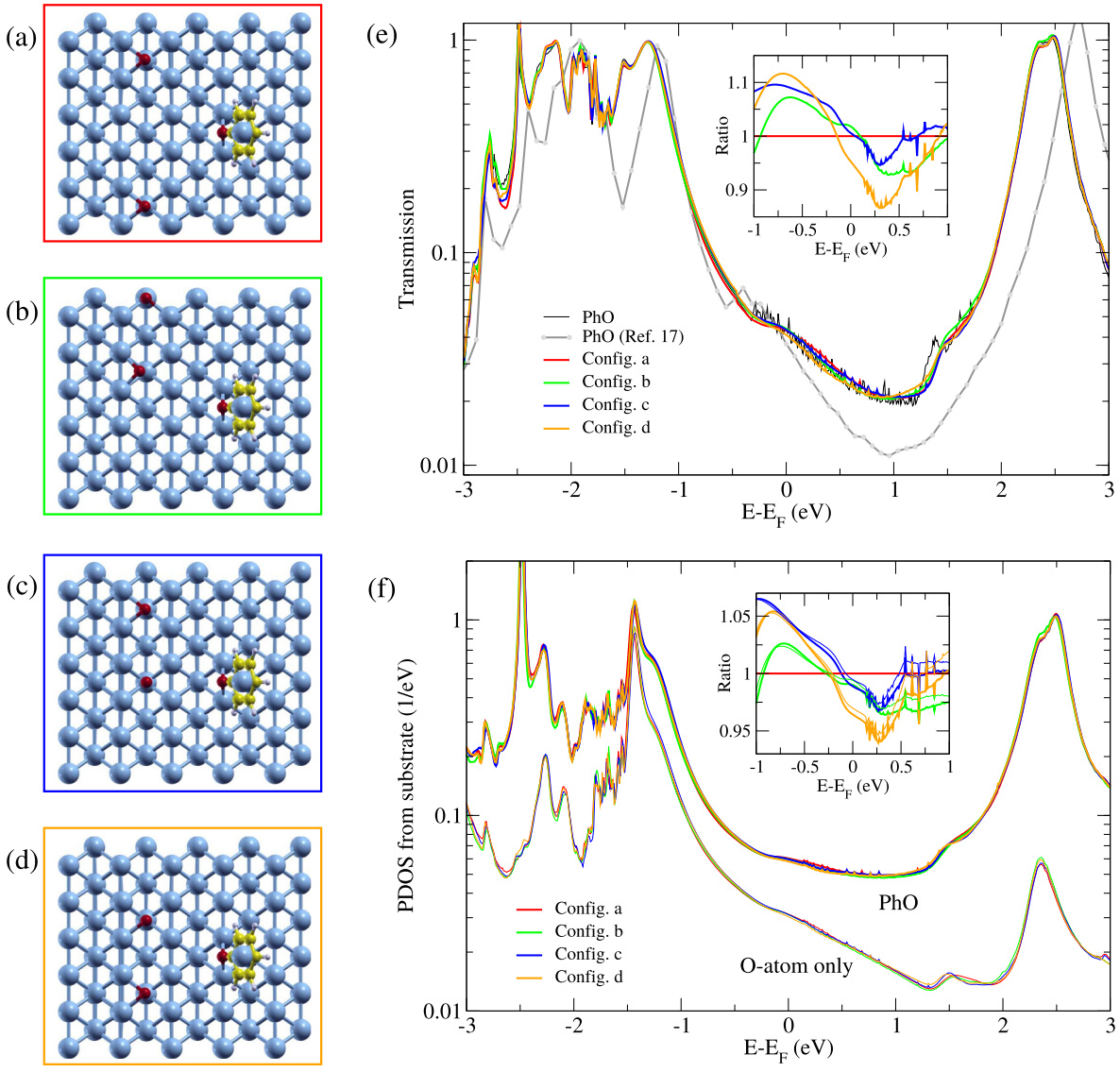

Fig. 6. Transport calculations for the PhO in the configurations shown in Fig. 3. (a)–(d) Top views of the different oxygen atom positions (only the tip apex atom is shown). (e) The colored curves show electron transmission for each of the configurations (a)–(d). The black curve shows transmission for isolated PhO using identical computational settings. The gray curve is the result from Ref. [17] based on a smaller unit cell and a slightly different computational approach. The inset shows the transmission ratios with respect to the configuration in panel (a), revealing a decreased transmission of about 5% at the Fermi level in configuration (d),(f) PDOS from the substrate electrode on the PhO atomic orbitals (thick lines) or on the anchoring O-atom only (thin lines). The PDOS ratios correlate well with the transmission ratios in panel (e). (For interpretation of the references to color in this figure legend, the reader is referred to the web version of this article.)

Acknowledgments

This work was supported by JSPS KAKENHI Grant Number JP16H00966. TF acknowledges FIS2017-83780-P from the Spanish Ministerio de Economía y Competitividad.

Supplementary material

Supplementary material associated with this article can be found, in the online version, at doi:10.1016/j.susc.2018.04.024.

References

[1] K. Morgenstern, N. Lorente, K.H. Rieder, Controlled manipulation of single atoms and small molecules using the scanning tunnelling microscope, Phys. Status Solidi B9 (2013) 1671–1751.
[2] W. Ho, Single-molecule chemistry, J. Chem. Phys. 117 (2002) 11033–11061.
[3] D.M. Eigler, C.P. Lutz, W.E. Rudge, An atomic switch realized with the scanning tunneling microscope, Nature 352 (1991) 600–603.
[4] L. Bartels, G. Meyer, K.H. Rieder, Basic steps of lateral manipulation of single atoms and diatomic clusters with a scanning tunneling microscope tip, Phys. Rev. Lett. 79 (1997) 697–700.
[5] L. Bartels, G. Meyer, K.H. Rieder, Controlled vertical manipulation of single CO molecules with the scanning tunneling microscope: a route to chemical contrast, Appl. Phys. Lett. 71 (1997) 213–215.
[6] J.R. Hahn, W. Ho, Single molecule imaging and vibrational spectroscopy with a chemically modified tip of a scanning tunneling microscope, Phys. Rev. Lett. 87 (2001) 196102.
[7] W. Haiss, C. Wang, I. Grace, A.S. Batsanov, D.J. Schiffrin, S.J. Higgins, M.R. Bryce, C.J. Lambert, R.J. Nichols, Precision control of single-molecule electrical junctions, Nature Mater. 5 (2006) 995–1002.
[8] L. Lafferentz, F. Ample, H. Yu, S. Hecht, C. Joachim, L. Grill, Conductance of a single conjugated polymer as a continuous function of its length, Science 323 (2009) 1193–1197.
[9] R. Temirov, A. Lassise, F.B. Anders, F.S. Tautz, Kondo effect by controlled cleavage of a single-molecule contact, Nanotechnology 19 (2008) 1–13.
[10] G. Reecht, F. Scheurer, V. Speisser, Y.J. Dappe, F. Mathevet, G. Schull, Electroluminescence of a polythiophene molecular wire suspended between a metallic surface and the tip of a scanning tunneling microscope, Phys. Rev. Lett. 112 (2014) 047403.
[11] D.M. Eigler, E.K. Schweizer, Positioning single atoms with a scanning tunnelling microscope, Nature 344 (1990) 524–526.

[12] M.F. Crommie, C.P. Lutz, D.M. Eigler, Confinement of electrons to quantum corrals on a metal surface, Science 262 (1993) 218–220.
[13] S.W. Hla, K.F. Braun, K.H. Rieder, Single-atom manipulation mechanisms during a quantum corral construction, Phys. Rev. B 67 (2003) 201402(R).
[14] G. Meyer, B. Neu, K.H. Rieder, Controlled lateral manipulation of single molecules with the scanning tunneling microscope, Appl. Phys. A 60 (1995) 343–345.
[15] F. Moresco, G. Meyer, K.H. Rieder, H. Tang, A. Gourdon, C. Joachim, Recording intramolecular mechanics during the manipulation of a large molecule, Phys. Rev. Lett. 87 (2001) 088302.
[16] L. Grill, K.H. Rieder, F. Moresco, G. Rapenne, S. Stojkovic, X. Boujou, C. Joachim, Rolling a single molecular wheel at the atomic scale, Nat. Nanotechnol. 2 (2007) 95–98.
[17] Y. Kitaguchi, S. Habuka, S. Hatta, H. Okuyama, T. Aruga, T. Frederiksen, M. Paulsson, H. Ueba, Controlled switching of single-molecule junctions by mechanical motion of a phenyl ring, Beilstein J. Nanotechnol. 6 (2015) 2088–2095.
[18] Y. Kitaguchi, S. Habuka, S. Hatta, H. Okuyama, T. Aruga, T. Frederiksen, M. Paulsson, H. Ueba, Controlling single-molecule junction conductance by molecular interactions, Sci. Rep. 5 (2015). 11796.
[19] Y. Kitaguchi, S. Habuka, T. Mitsui, H. Okuyama, S. Hatta, T. Aruga, Comparative study of phenol and thiophenol adsorption on Cu(110), J. Chem. Phys. 139 (2013) 044708.
[20] B.G. Briner, M. Doering, H.P. Rust, A.M. Bradshaw, Mobility and trapping of molecules during oxygen adsorption on Cu(110), Phys. Rev. Lett. 78 (1997) 1516–1519.
[21] T. Kumagai, M. Kaizu, H. Okuyama, S. Hatta, T. Aruga, I. Hamada, Y. Morikawa, Tunneling dynamics of a hydroxyl group adsorbed on Cu(110), Phys. Rev. B 79 (2009). 035423.
[22] J.M. Soler, E. Artacho, J.D. Gale, A. García, J. Junquera, P. Ordejón, D. Sánchez-Portal, The SIESTA method for ab initio order-n materials simulation, J. Phys.: Condens. Matter 14 (2002) 2745–2779.
[23] M. Dion, H. Rydberg, E. Schroder, D.C. Langreth, B.I. Lundqvist, Van der waals density functional for general geometries, Phys. Rev. Lett. 92 (2004) 246401.
[24] K. Lee, E.D. Murray, L. Kong, B.I. Lundqvist, D.C. Langreth, Higher-accuracy van der waals density functional, Phys. Rev. B 82 (2010) 081101.
[25] G. Roman-Perez, J.M. Soler, Efficient implementation of a van der waals density functional: application to double-wall carbon nanotubes, Phys. Rev. Lett. 103 (2009) 096102.
[26] M. Brandbyge, J.L. Mozos, P. Ordejón, J. Taylor, K. Stokbro, Density-functional method for nonequilibrium electron transport, Phys. Rev. B 65 (2002) 165401.
[27] N. Papior, N. Lorente, T. Frederiksen, A. García, M. Brandbyge, Improvements on non-equilibrium and transport green function techniques: the next-generation tranSIESTA, Comp. Phys. Commun. 212 (2017) 8–24.
[28] N.J. Tao, Electron transport in molecular junctions, Nat. Nanotechol. 1 (2006) 173–181.
[29] H. Haick, D. Cahen, Making contact: connecting molecules electrically to the macroscopic world, Prog. Surf. Sci. 83 (2008) 217–261.
[30] M. Kiguchi, S. Kaneko, Single molecule bridging between metal electrodes, Phys. Chem. Chem. Phys. 15 (2013) 2253–2267.
[31] H. Basch, R. Cohen, M.A. Ratner, Interface geometry and molecular junction conductance: geometric fluctuation and stochastic switching, Nano Lett. 5 (2005) 1668–1675.
[32] L. Venkataraman, J.E. Klare, C. Nuckolls, M.S. Hybertsen, M.L. Steigerwald, Dependence of single-molecule junction conductance on the molecular conformation, Nature 442 (2006) 904–907.
[33] C.M. Guédon, H. Valkenier, T. Markussen, K.S. Thygesen, J.C. Hummelen, S.J. van der Molen, Observation of quantum interference in molecular charge transport, Nat. Nanotechnol. 7 (2012) 305–309.
[34] F. Chen, X. Li, J. Hihath, Z. Huang, N. Tao, Effect of anchoring groups on single-molecule conductance: comparative study of thiol-, amine-, and carboxylic-acid-terminated molecules, J. Am. Chem. Soc. 128 (2006) 15874–15881.
[35] M. Kiguchi, H. Nakamura, Y. Takahashi, T. Takahashi, T. Ohto, Effect of anchoring group position on formation and conductance of a single disubstituted benzene molecule bridging Au electrodes: change of conductive molecular orbital and electron pathway, J. Phys. Chem. C 114 (2010) 22254–22261.
[36] C.R. Arroyo, E. Leary, A. Castellanos-Gómez, G. Rubio-Bollinger, M.T. González, N. Agraït, Influence of binding groups on molecular junction formation, J. Am. Chem. Soc. 133 (2011) 14313–14319.
[37] Y. Selzer, L. Cai, M.A. Cabassi, Y. Yao, J.M. Tour, T.S. Mayer, D.L. Allara, Effect of local environment on molecular conduction: isolated molecule versus self-assembled monolayer, Nano Lett. 5 (2005) 61–65.
[38] V. Fatemi, M. Kamenetska, J.B. Neaton, L. Venlataraman, Environmental control of single-molecule junction transport, Nano Lett. 11 (2011) 1988–1992.
[39] N. Néel, J. Kröger, L. Limot, T. Frederiksen, M. Brandbyge, R. Berndt, Controlled contact to a C_{60} molecule, Phys. Rev. Lett. 98 (2007) 065502.
[40] J. Kröger, N. Néel, L. Limot, Contact to single atoms and molecules with the tip of a scanning tunnelling microscope, J. Phys.: Condens. Matter 20 (2008) 223001.
[41] G. Schulze, K.J. Franke, A. Gagliardi, G. Romano, C.S. Lin, A.L. Rosa, T.A. Niehaus, T. Frauenheim, A.D. Carlo, A. Pecchia, J.I. Pascual, Resonant electron heating and molecular phonon cooling in single C_{60} junctions, Phys. Rev. Lett. 100 (2008) 136801.
[42] Y.F. Wang, J. Kröger, R. Berndt, H. Vázquez, M. Brandbyge, M. Paulsson, Atomic-scale control of electron transport through single molecules, Phys. Rev. Lett. 104 (2010) 176802.
[43] R. Berndt, J. Kröger, N. Néel, G. Schull, Controlled single atom and single molecule contacts, Phys. Chem. Chem. Phys. 12 (2010) 1022–1032.
[44] R. Hiraoka, R. Arafune, N. Tsukahara, M. Kawai, N. Takagi, Transport characteristics of a single c_{60}-molecule junction revealed by multiple Andreev reflections, Phys. Rev. B 90 (2014) 241405(R).
[45] R.J. Nichols, S.J. Higgins, Single-molecule electronics: chemical and analytical perspectives, Annu. Rev. Anal. Chem. 8 (2015) 389–417.
[46] J. Brand, P. Ribeiro, N. Néel, S. Kirchner, J. Kröger, Impact of atomic-scale contact geometry on Andreev reflection, Phys. Rev. Lett. 118 (2017) 107001.
[47] P.J. Feibelman, D.R. Hamann, Electronic structure of a ”poisoned” transition-metal surface, Phys. Rev. Lett. 52 (1984) 61–64.
[48] I. Hamada, T. Kumagai, A. Shiotari, H. Okuyama, S. Hatta, T. Aruga, Nature of hydrogen bonding in hydroxyl groups on a metal surface, Phys. Rev. B 86 (2012) 075432.